2015-01-01

AC-Susceptibility and EPR Investigations of Superspin Dynamics in Magnetite Nanoparticles

Alex D. Price
University of Texas at El Paso, adprice@miners.utep.edu

AC SUSCEPTIBILITY AND EPR INVESTIGATIONS OF SUPERSPIN DYNAMICS IN MAGNETITE NANOPARTICLES

ALEX D. PRICE

Department of Physics

APPROVED:

Cristian Botez, Ph.D., Chair

Russell R. Chianelli, Ph.D.

Rosa Fitzgerald, Ph.D.

Charles Ambler, Ph.D.
Dean of the Graduate School

Dedication

To my parents

Fred and Laura Price

for their love, friendship, and support.

AC SUSCEPTIBILITY AND EPR INVESTIGATIONS OF SUPERSPIN DYNAMICS IN MAGNETITE NANOPARTICLES

by

ALEX D. PRICE

THESIS

Presented to the Faculty of the Graduate School of

The University of Texas at El Paso

in Partial Fulfillment

of the Requirements

for the Degree of

MASTER OF SCIENCE

Department of Physics

THE UNIVERSITY OF TEXAS AT EL PASO

August 2015

Acknowledgements

I would like to thank Dr. Cristian E. Botez for his guidance of my research work, his suggestions throughout the project, and for the opportunities he has given to me. I would like to express my gratitude towards Dr. Russell Chianelli and Dr. Rosa Fitzgerald for their help regarding this thesis. My thanks to Dr. Sohan de Silva, for his assistance and guidance in various aspects of this research. My special thanks to my friends and family, for their love, friendship, and encouragement. I would also like to extend a special thank you to The Leo, for his support and irreplaceable friendship.

Abstract

In this investigation we use two complementary techniques to distinguish between superparamagnetic blocking (SPB) and superspin-glass (SSG) freezing phenomena in magnetite nanoparticles. While these manifestations of the superspin dynamics are fundamentally different, they have similar "signatures", especially in dc-magnetization experiments. Even if ac-susceptibility measurements are employed, careful use of mathematical models to analyze the data are needed to uncover which type of phenomena (SPB or SSG freezing) occurs within the material. Yet, by utilizing electron paramagnetic resonance (EPR) on a 10 nm Fe_3O_4 nano-powder as well as on a ferrofluid (based on the same nanoparticle ensemble) we found a very distinct difference in the absorption spectra between the two samples, which indicates markedly different EPR signatures from SPB and SSG freezing behaviors.

Table of Contents

List of Figures

Chapter 1: Introduction

Nanoscience, in general, is defined as the study of physical properties of materials and phenomena when the particle size is on the scale of 1 – 100 nm. The magnetic domains within the material are responsible for the various behaviors magnetic materials exhibit. In recent studies of science and technology, magnetic nanoparticles are showing potential in the development of high density storage [1] and in biomedicine, such as cancer treatments [2].

1.1 MAGNETIC NANOPARTICLES

Magnetic materials, due to their intriguing properties, have been implemented in various types of devices since ancient times. From early times, lodestones have been used in magnetic compasses for navigation [3]. Currently, with the advent of nanoscience and nanotechnology in the 1980s, nanomaterials have become an important and exciting field of study. Nanomagnetism, the study of magnetic nanoparticles, is a strong topic for today's scientists. The determination of magnetic properties in nanomaterials are due to several factors, one of which being the particle size [4]. When the size of the particle becomes small enough, the magnetic domains in the material become defined by the particle rather than a grouping of particles with similar magnetic alignment as seen in bulk materials. There still isn't a full understanding as to the behavior of the material between these two extremes which has led to current research and extensive studies of magnetic nanoparticles.

1.2 MAGNETITE

Magnetite is an abundantly naturally occurring mineral with strong magnetic properties and several different types of applications. Such applications are audio recording devices that were developed by coating tape with magnetite powder [5] as well as an arsenic sorbent for water purification [6]. Magnetite, chemically defined as Fe_3O_4, is a mineral belonging to the spinel group and the most magnetic naturally occurring mineral on Earth [7].

1.3 FERROFLUIDS

Ferrofluids are colloidal substances comprised of ferromagnetic or ferrimagnetic nanoscale particles suspended in a carrier fluid. It was developed in 1963 by Steve Papell at NASA in order to draw rocket fuel to a pump inlet when in a weightless environment [8]. This liquid, when subjected to the presence of a magnetic field, becomes strongly magnetized. However, they typically do not retain magnetization when there is no external magnetic field giving them the classification of superparamagnets instead of ferromagnets [9]. They have many applications ranging from its use in art, such as liquid sculptures by Sachiko Kodama [10], analytical instrumentation due to its refractive properties, and even medical science, such as magnetic hyperthermia [2].

Chapter 2: Theoretical Background

2.1 MAGNETIZATION

We are looking to describe the magnetic behavior of magnetite nanoparticles for this study. Therefore, it is appropriate to summarize the known types of magnetic behavior. The initial cause of magnetization in materials shall also be briefly explained, so as to tie in the cause and effect of magnetism within the material world.

2.1.1 Origins

The earliest mention of magnetism is roughly around 600 B.C. with a statement by Thales of Miletus who said a lodestone attracts iron because it has a soul [11]. Yet, it hasn't been until the twentieth century that scientists have begun to understand it and apply that understanding to science and technology that is used even today. The definition of magnetism stems out from electrodynamics and quantum mechanics.

Magnetism is generated in matter by the combination of an electron's orbital angular momentum and intrinsic spin. Together they form the magnetic dipole moment which gives rise to a magnetic field. Although it is theoretically shown that any particle with an electric charge can generate a magnetic field, the net contribution can sometimes be negligible and thus ignored, such as in the case of the nucleus of an atom.

The magnetic dipole consists of a north and a south pole. These two poles are attracted to each other and, in the simple case of two dipoles, align oppositely in almost every case when within a close proximity to one another. However, in the case of electrons, the Pauli Exclusion Principle shows that two dipoles can be aligned in a parallel fashion. In fact, the electrostatic interaction energy of the parallel alignment is lower than that of the oppositely aligned case. This can be described by the exchange energy.

The exchange interaction is purely quantum mechanical in nature and has no classical counterpart. It describes the change of the position or energy expectation value due to the exchange symmetry of the wave function of indistinguishable particles. Fermions experience this

due to the Pauli Exclusion Principle in the form of Pauli repulsion which is responsible for keeping electrons with identical spin away from each other. This can also be seen as an attraction, in the case of bosons, which gives rise to phenomena such as the Bose-Einstein Condensate. This quantum mechanical effect is the main cause for the ordering of magnetic moments in magnetic materials.

Magnetization is a physical quantity proportional to the magnetic moment of a particle or collection of particles. The magnetic susceptibility of a material is then defined by the level of magnetization that responds to the presence of an applied magnetic field. Most materials are classified as linear magnetic materials, where the magnetic susceptibility is defined as:

$$\boldsymbol{M} = \chi \boldsymbol{H} \tag{1}$$

where **M** is the magnetization, χ is the magnetic susceptibility, and **H** is the magnetic field strength. Depending on the value of χ, being positive or negative, a material can be classified as paramagnetic or diamagnetic, respectively.

2.1.2 Magnetic Domains

A region within a magnetic material consisting of a magnetization in a uniform direction is called a magnetic domain. The net magnetization of the material is the collection of the magnetic domains under the principle of superposition. The space between magnetic domains is referred to as the domain wall, which is comprised of the magnetization with a coherent rotation between the two magnetic domains. In a sample that has no magnetization, these domains are randomly oriented, yet when an external magnetic field is applied, the magnetic domains can be aligned and thus a net magnetization of the material is registered, as shown in figure 2.1. These domains tend to align with a sufficiently strong applied external magnetic field, causing the domain sizes to change in favor of the applied field.

There is a particularly interesting property to the magnetic domain when in the nanoscale world. When the particle size becomes smaller than some critical size, each particle will act as its own magnetic domain. This causes rise to potentially different magnetic behavior compared to its bulk counterpart such as superparamagnetism.

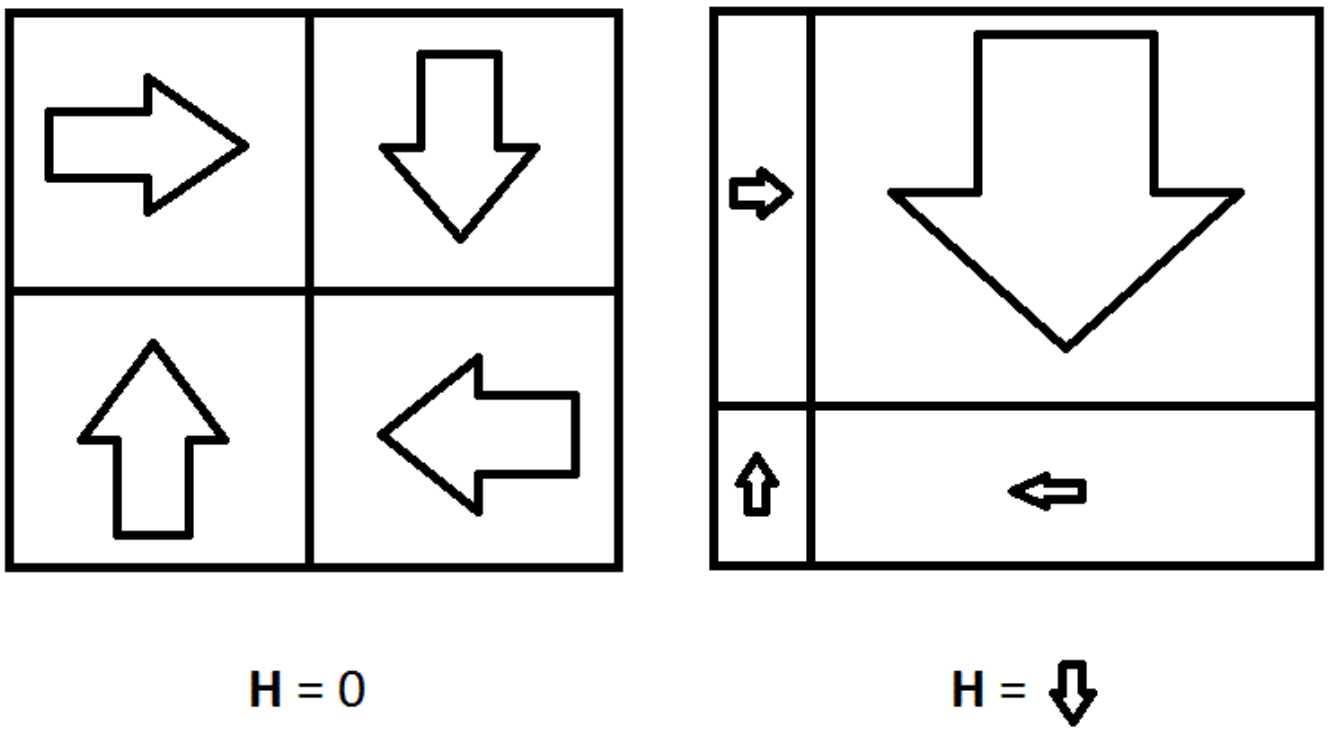

Figure 2.1 – Magnetic Domain Behavior

2.1.3 Diamagnetism

Diamagnetism is a property of all matter, though it is usually weak compared to other types of magnetization. When an external magnetic field is applied to a material, the materials response to oppose that external field is diamagnetism. In diamagnetic materials, there is an absence of unpaired electrons and the atoms or molecules that comprise the material have no net angular momentum. The magnetization due to an external field is thus a property of the electrons' orbital motions.

2.1.3 Ferromagnetism

A ferromagnetic material has unpaired electrons within the atoms. Compared to diamagnetism, this allows for a stronger magnetization. The unpaired electrons' magnetic moments align parallel to the applied field, yet, when the applied field is removed, the electrons have a tendency to stay aligned parallel to each other. Ferromagnetism is probably one of the oldest known forms of magnetism, as well as common in our everyday life. Refrigerator magnets, bar magnets, and horseshoe magnets are examples of ferromagnets. The ions within a ferromagnetic material will align in such a way to contribute in appositive manner to the net magnetization resulting in a total alignment of the magnetic moments, whereas in a ferrimagnetic material there is a partial alignment since some of the magnetic moments will align oppositely, yielding a lower net magnetization. In antiferromagnetic materials, the magnetic moments align in such a way that there is no net magnetization (Fig 2.2).

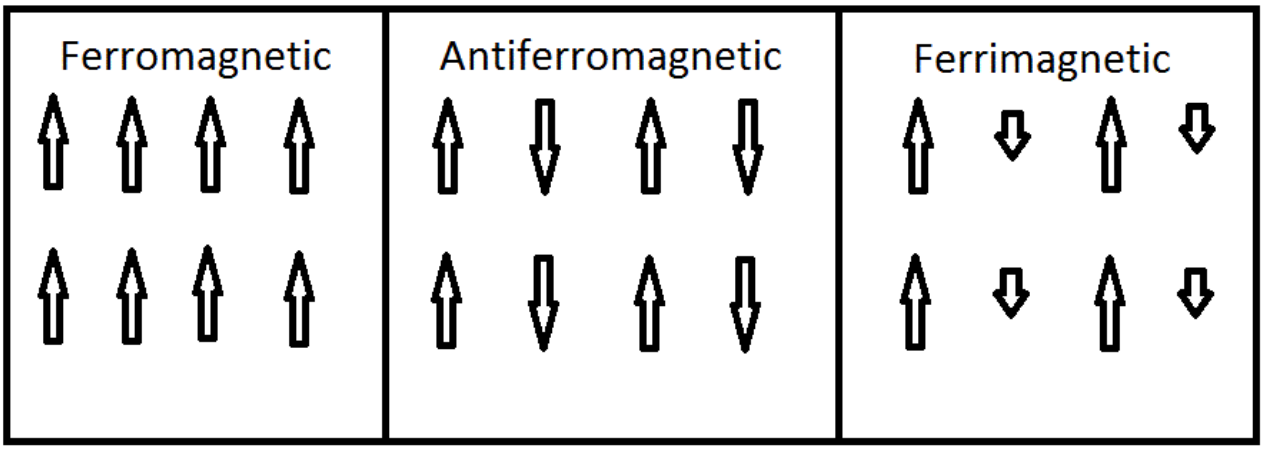

Figure 2.2 – Ferromagnetic, Antiferromagnetic, and Ferrimagnetic Behavior

Every ferromagnet has its own temperature, which, when exceeded, will lose its ferromagnetic properties. This is known as the Curie temperature. Once a ferromagnetic material is above that temperature limit, the internal thermal energy overcomes the dipole interaction energy, thus allowing the dipoles to move and align freely within the material.

2.1.4 Paramagnetism

Another, fairly common knowledge, type of magnetism is paramagnetism. Paramagnetic materials behave similarly to ferromagnetic materials when an external magnetic field is applied, however, the magnetic moments will not stay aligned when the external field is removed. A paramagnet is the result of a material whose internal thermal energy is sufficiently high enough to overcome the interaction energy between dipoles, given that there is no external magnetic field.

In ferromagnetic materials whose size is around some critical size, typically nanoscale, the magnetic domains will begin to exhibit interesting behavior. The magnetic moments within a particle will align, in their entirety, in the same direction. Each particle becomes a single magnetic domain, essentially acting as its own individual, gargantuan magnetic moment. As in paramagnetic materials, there will be a particular temperature that will allow these single particle domains to rotate freely and align with an external magnetic field, should one be applied. Should the temperature drop below this critical temperature, then the particles will be unable to rotate freely and is said to be blocked. This phenomenon is known as superparamagnetism [12].

2.1.5 Superparamagnetic Blocking

Each material has its own specific temperature where the single-domain nanoparticles transition from a fixed, or blocked, state to a freely rotating superparamagnetic state. This temperature is known as the blocking temperature:

$$T_B = \frac{KV}{k_B ln\left(\frac{\tau_m}{\tau_0}\right)} \tag{2}$$

where K is the nanoparticle's magnetic anisotropy energy density and V is the volume, k_B is the Boltzmann constant, τ_m is the measurement time, and τ_0 is the attempt time which is characteristic of the material typically with a value of 10^{-9} - 10^{-12} seconds. The quantity KV is the energy barrier. The measurement time is viewed in conjunction with the Néel relaxation time, τ_N, which defines the mean time between spontaneous flips of the magnetic moment. When the

measurement time is above the relaxation time, the material is in a superparamagnetic state and when the measurement is below, the material is in a blocked state.

2.1.6 Spin-glass

A spin-glass is a material with a disordered configuration of magnetic moments. In essence, the magnetic disorder is analogous to that of a chemical glass, but rather with spin configurations instead of positional disorder. Due to this frozen-in structural disorder, no long range order can be established, such as with ferromagnetism or anti-ferromagnetism [13]. This conflicted ordering between magnetic moments leads to a net magnetization of zero, when not in an external magnetic field. In essence, there is a similarity to the disorder found in a paramagnet, except instead of the dynamic disorder the material has a static disorder.

When the particle size is sufficiently small, superspin-glass behavior may be exhibited. This is essentially the same as a traditional spin-glass, yet has a similar relationship much as the superparamagnet has with a paramagnet. The constituent particles are single domain ferromagnetic clusters when looking at a superspin-glass, as opposed to atomic dipoles when dealing with a spin-glass.

2.2 MAGNETIC BEHAVIOR

A material's overall magnetic behavior depends on the structure of the material, particularly its electronic configuration. In general, this is expressed in terms of energy barriers and/or constraints. Should a material be supplied enough energy, typically thermal, the barriers/constraints can be overcome thus allowing the material to transition into a different type of magnetic behavior. As such, there are magnetic transitions that are material specific, along with their corresponding temperatures that these transitions arise.

There are many theories and models that can be used to show these magnetic phase transitions. Common practice is to fit the magnetic transition data for a material to a corresponding mathematical model. Though there are several models, this investigation will only delve into those that are related our nanoparticles.

2.2.1 Curie Law

Pierre Curie is mostly known for his doctoral studies on magnetism. During his studies on ferromagnetism, paramagnetism, and diamagnetism, he experimentally discovered the temperature dependence of paramagnets which has become known as Curie's Law:

$$\boldsymbol{M} = C * \frac{\boldsymbol{B}}{T} \tag{3}$$

where **M** is the net magnetization, **B** is the magnetic field, T is the absolute temperature, and C is the Curie constant for the material. What can be seen from this is that the magnetization of a given material is proportional to an applied external field; however, this proportion is diminished upon heating the material. Curie's law only holds for high temperatures or weak magnetic fields. If the temperature is sufficiently low, there won't be enough thermal energy to create magnetic disorder. Similarly, should the applied field be sufficiently strong, the magnetic moments will align with the field in their entirety.

2.2.2 Curie and Néel Points

Magnetic dipoles' interactions and ability to align in parallel are governed not only by the distance between them; energy dependencies, such as entropy, may also overcome the tendency for alignment. Given enough thermal energy, the coupling forces between dipoles may be overcome, such as those in a ferromagnet. In essence, there is temperature dependence for the magnetic alignment within the material.

In a ferromagnet, this temperature, called the Curie temperature, dictates the transition between two types of magnetic behaviors. For temperatures below the Curie temperature, a ferromagnet behaves as expected; the magnetic moments will align with each other and give a net magnetization that is non-zero for the material when in the absence of an applied magnetic field. However, above the Curie point, the thermal energy is sufficient enough to cause the magnetic dipoles at arrange themselves in a random fashion, unless subjected to an applied field which will cause them to align. Therefore, the Curie temperature dictates a ferromagnetic material's transition from a permanent magnet to an induced magnet or paramagnet. As an

analog to the Curie temperature, there is the Néel temperature, which explains a similar phenomenon for when antiferromagnetic material transitions to that of a paramagnet.

2.2.3 Néel – Brown Theory

Néel – Brown theory, otherwise known as Néel – Arrhenius theory or Néel relaxation theory, explains "magnetic viscosity," a time-dependent magnetic phenomena in which the magnetic domain alignment of a material responds with a time lag to an applied magnetic field. The theory was first developed by Louis Néel [14] and later refined, through rigorous derivation, by William Fuller Brown, Jr. [15]. The theory describes the magnetic response of material comprised of single-domain ferromagnets; where each particle acts as a single domain giving each particle a very large magnetic moment.

The magnetic anisotropy of the nanoparticle separates the stable orientations of the magnetic moment by an energy barrier. These stable orientations are defined by an "easy axis", which is a material's natural alignment of the magnetic moments. This directional dependence is the preferred alignment of spontaneous magnetization. The energy barrier defines the energy needed in order to change the direction of magnetization, by changing the direction of magnetization from an "easy axis" through a "hard axis" and resting at another "easy axis", and is dependent on material specific properties as well as the particle size. Therefore, should the size of the nanoparticle change, so shall the energy needed to overcome the energy barrier, in addition to the critical temperature which the material begins to give a superparamagnetic response.

The Néel – Arrhenius equation is used to show the average length of time it takes for a ferromagnetic moment to randomly flip due to the thermal fluctuations in the material:

$$\tau_N = \tau_0 e^{\left(E/k_B T\right)} \tag{4}$$

where τ_N is the average time for the spin to flip due to thermal fluctuations, τ_0 is a constant called the attempt time, a characteristic of the material that is generally of the order $10^{-9} – 10^{-12}$ s, E is the magnetic anisotropy energy, k_B is the Boltzmann constant, and T is the absolute temperature.

The energy barrier E = KV, where K is the anisotropy energy density and V is the volume, thus showing the particle size dependence of the energy barrier. Hence, should the size of the particle increase, so shall the energy needed to change its magnetic orientation, leading to a longer transition time from magnetic alignment with the recently applied external field to a randomized configuration. It is key to note that this law describes a system of non-interacting nanoparticles with a random magnetic orientation.

When the temperature of the material is above a critical temperature, known as the blocking temperature, there is enough thermal energy to allow the nanoparticles to align with an external field. However, below the blocking temperature, the nanoparticles will not be responsive enough to the applied field; in particular, the relaxation time will be greater than the attempt time. This will be the blocked state of the material, as the magnetization will not have changed in the required timeframe from that of its original configuration.

2.2.3 Vogel-Fulcher Law

Another law that describes magnetic relaxation is the Vogel – Fulcher activation law, which is similar to the Néel – Arrhenius equation. This usage was proposed by Shtrikman and Wohlfarth [16] and by Tholence [17] as a model for spin glass relaxations.

The major difference between these equations is the Vogel – Fulcher activation law does account for some slight inter-particle interaction, making it useful for weakly interacting systems. The Vogel – Fulcher equation takes on a form similar to that of the Néel – Arrhenius equation:

$$\tau = \tau_0 e^{\left(E/(k_B(T-T_0))\right)} \tag{5}$$

where τ is the average time taken for a spin to flip directions due to thermal fluctuations, τ_0 is the attempt time, E is the magnetic anisotropy energy, k_B is the Boltzmann constant, T is the absolute temperature, and T_0 is the material specific characteristic temperature which accounts for the inter-particle interactions.

2.2.4 Power Law

In cases with high particle concentration, the effects of inter-particle interaction have an impact on the magnetic phase transition about the Curie point. Rather than individually blocking, the superspins freeze in a spin-glass fashion when cooled below a critical temperature [18-20]. This power activation law will be briefly described, as its derivation is outside the scope of this investigation.

Conventional dynamic scaling theory dictates that the relaxation time τ for a system diverges as a power law with the correlation length ξ, such that $\tau = \tau_0 \xi^z$, where z is the dynamic scaling exponent. The correlation length is defined as a parameter that deals with the average magnetic domain size. According to the static scaling hypothesis, parameters such as the correlation length and time should diverge, and the magnetization should diminish proportionally to the value of the reduced temperature to the related dynamic exponent. The correlation length becomes defined as:

$$\xi = \left(\frac{T}{T_G} - 1\right)^{-\nu} \tag{6}$$

where ξ is the correlation length, T is the temperature, T_G is the material specific spin-glass freezing temperature, and ν is a critical exponent. Combining this with the base form for the power law, the power law takes on the form:

$$\tau = \tau_0 \left(\frac{T}{T_G} - 1\right)^{-z\nu} \tag{7}$$

where $z\nu$ becomes the critical exponent. This power law is used for data fitting, just as the Néel – Arrhenius and Vogel – Fulcher equations are used.

Chapter 3: Experimental Methodology

3.1 MAGNETOMETRY

Prior magnetization measurements of 10 nm Fe_3O_4 were carried out on a Quantum Design® Physical Property Measurement System (PPMS) [21]. The PPMS was used to perform DC-magnetization measurements along with AC-susceptibility measurements. Figure 3.1 provides a visualization of the chamber configuration of the PPMS.

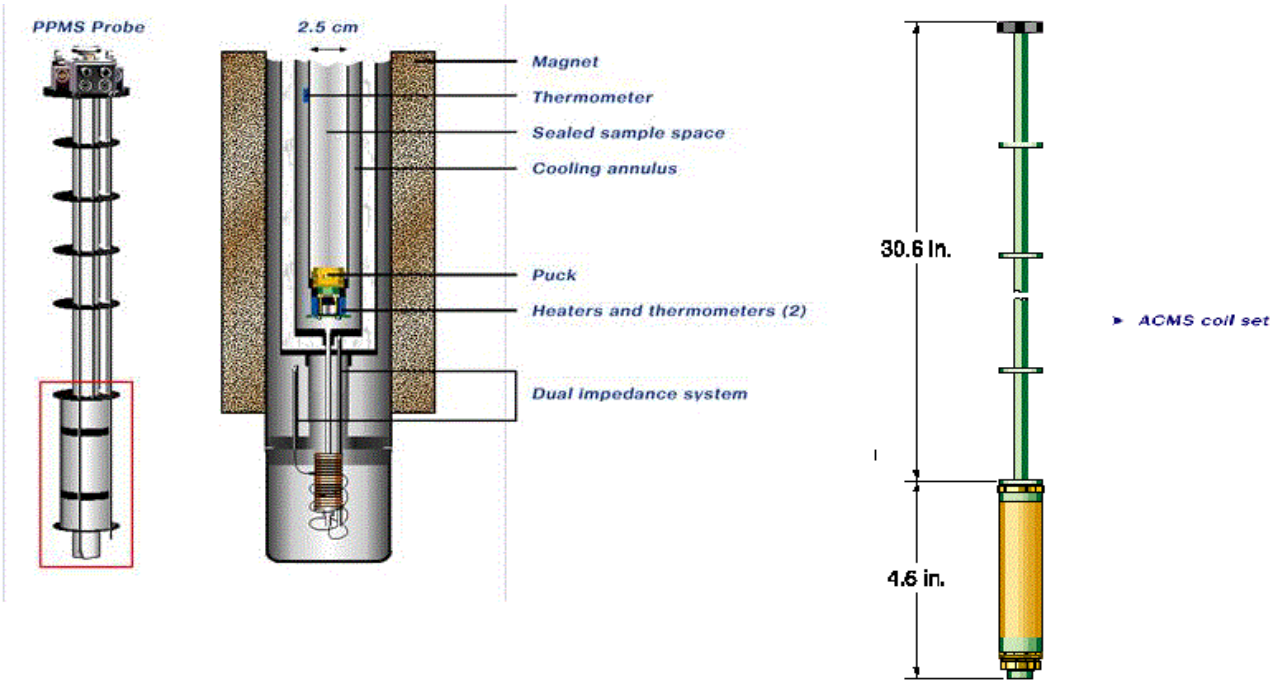

Figure 3.1 – PPMS Inner-Chamber Configuration

DC-magnetization measurements are carried out by lowering a sample into the coil assembly and applying a direct current. Zero-field-cooled (ZFC) measurements were taken by cooling the sample via liquid helium to the starting temperature (about 4 K). The coil assembly is raised and lowered by the motor system in order to induce a current which is then measured. The magnetization of the material is recorded in the presence of a constant field with an increasing temperature. Field-cooled (FC) measurements are taken in a similar fashion, although the sample is cooled while in the presence of a constant field as opposed to not. Previous

measurements from our lab, performed by Botez and Morris [21], indicate superparamagnetic relaxation in 10 nm magnetite nanoparticles. The field used for the FC and ZFC measurements was set to 50 Oe with temperatures starting as low as 4 K and increasing to 140 K for a 10 nm Fe_3O_4 powder (Figure 3.2). This shows the temperature dependence of the DC-magnetization collected upon heating an ensemble of magnetite nanoparticles in an external field of 50 Oe using FC and ZFC protocol [21].

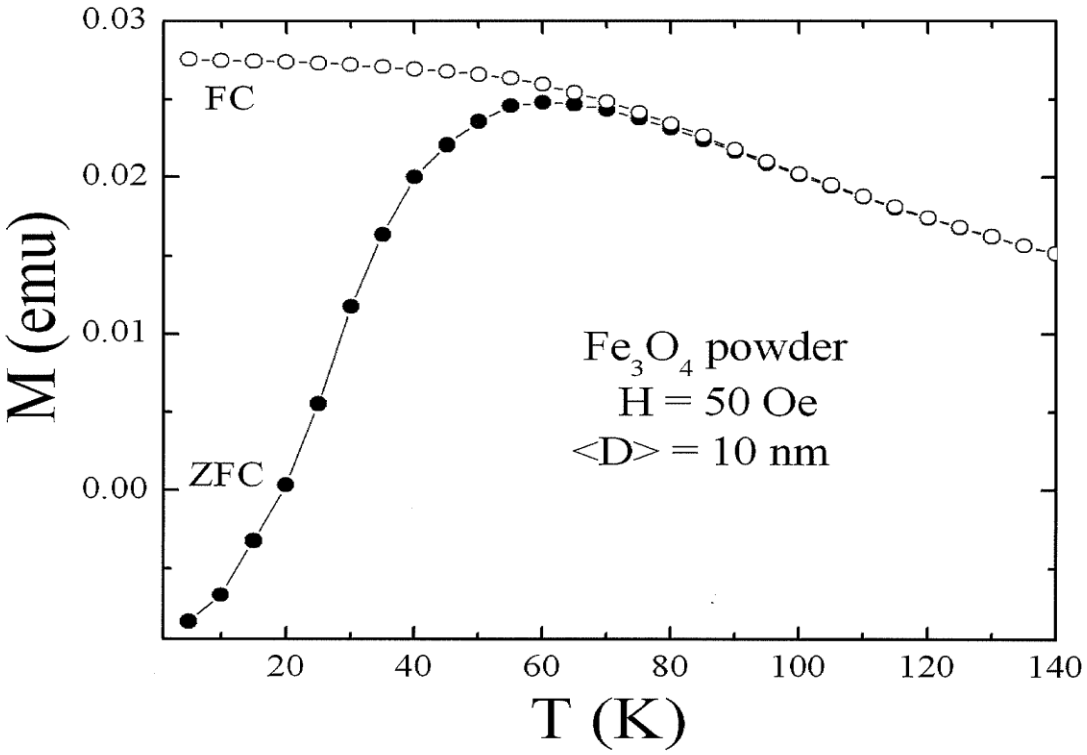

Figure 3.2 – FC and ZFC Measurements of Fe_3O_4 10 nm Nanoparticles

AC-susceptibility measurements were also taken for the 10 nm Fe_3O_4 powder as well as a 10 nm Fe_3O_4 ferrofluid with hexane used as the carrier fluid. The AC-susceptibility measurements are similar to that of DC-magnetization; however a small AC magnetic field is added to the constant DC field, hence giving the resultant superimposed field time dependency.

Thus, the magnetic moment of the sample produces a current in the induction coil. The moment that is produced by the superimposed field is the AC magnetic moment. The temperature dependence for the powder and the ferrofluid are measured with different frequencies, with the oscillating magnetic field amplitude of 5 Oe, as low as 100 Hz up to 10000 Hz (Figures 3.3 & 3.4) [21].

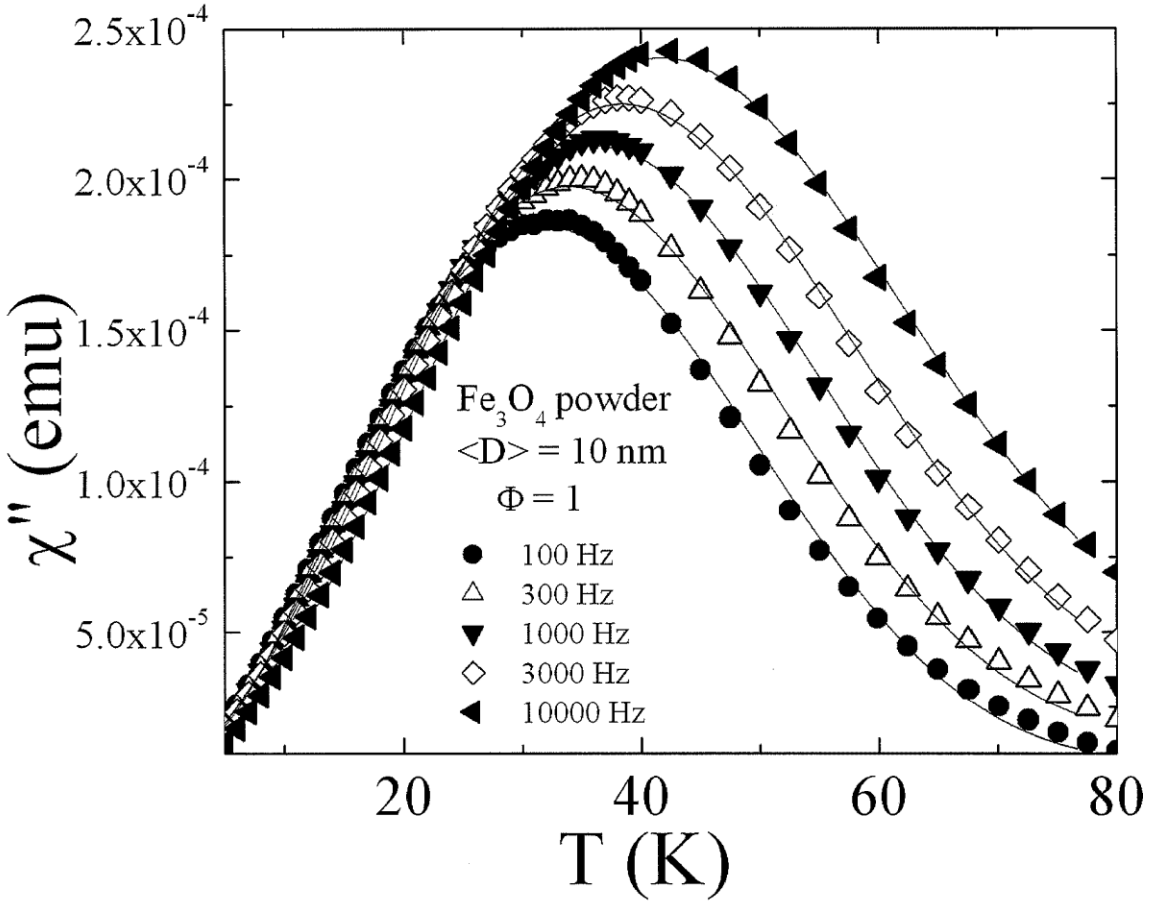

Figure 3.3 – AC-Susceptibility Measurements of Fe_3O_4 10 nm Nanopowder

These curves show the temperature dependence of the out-of-phase magnetic susceptibility collected at five different frequencies: 100 Hz, 300 Hz, 1000 Hz, 3000 Hz, and 10000 Hz. This was done similarly for the 10 nm magnetite ferrofluid.

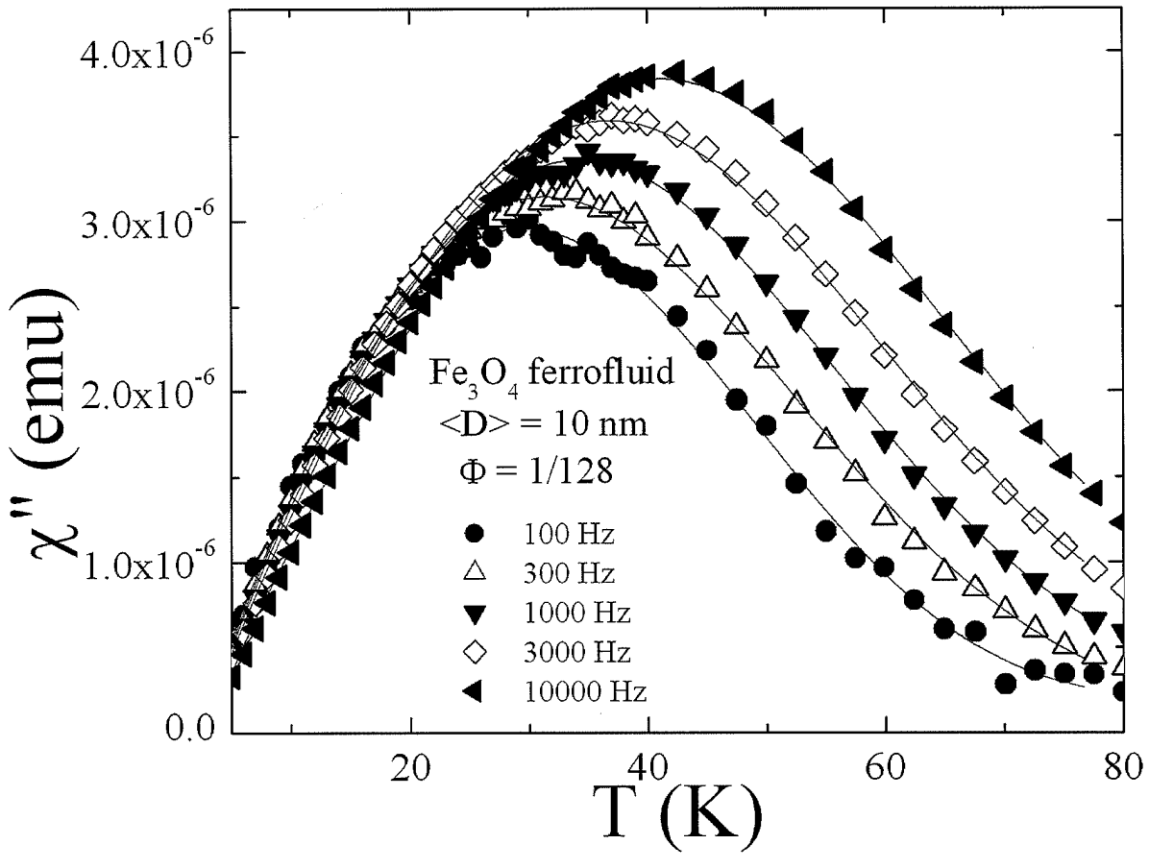

Figure 3.4 – AC-Susceptibility Measurements of Fe_3O_4 10 nm Ferrofluid

The transition states of the material, whether superparamagnetic blocking (SPB) or superspin-glass (SSG) freezing, are difficult to tell apart, therefore the peaks of the measurement data are then fit to mathematical models in order to define which behavior the material exhibits. Utilizing the Vogel – Fulcher activation law and the power activation law, the observation time dependence can be seen (Figures 3.5 & 3.6) [21].

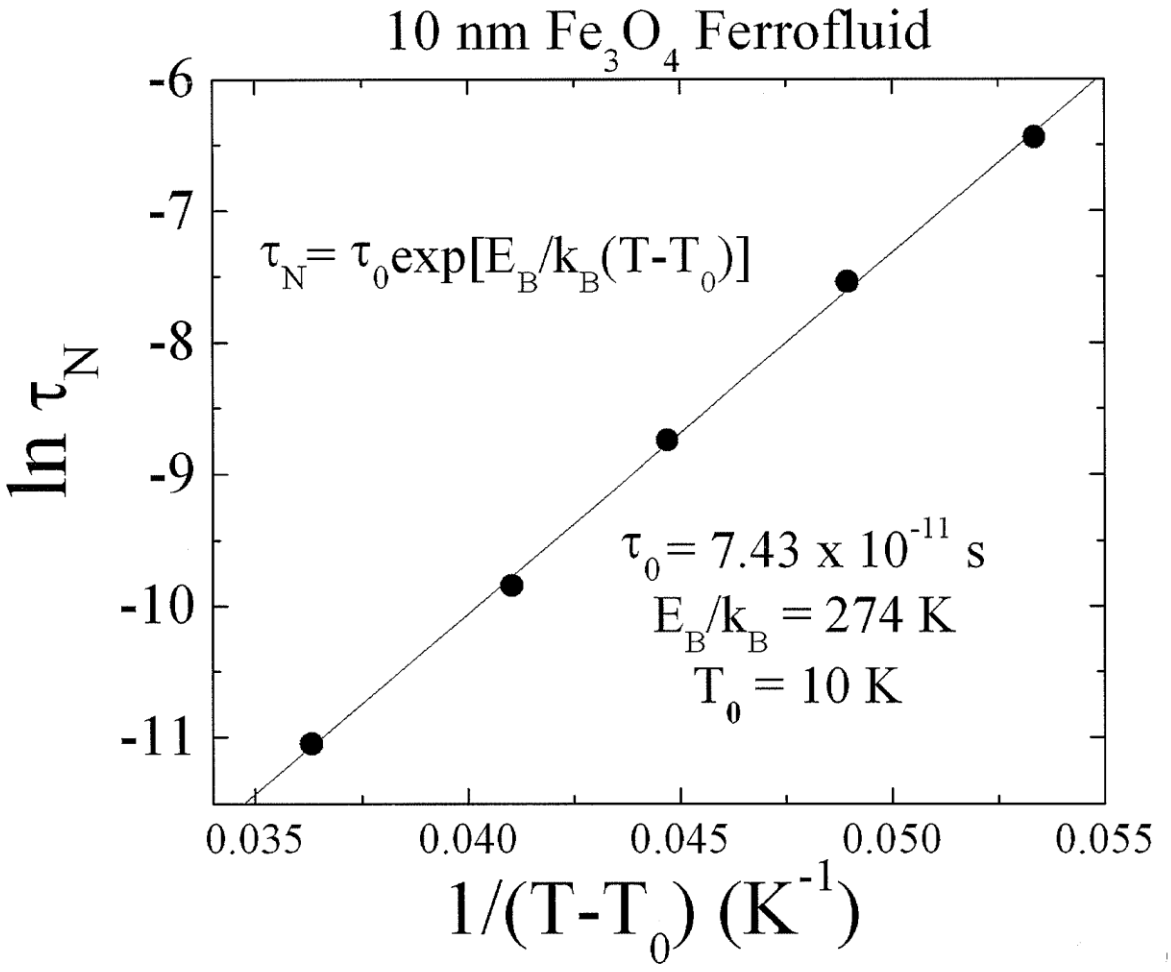

Figure 3.5 – Time Dependence of Fe_3O_4 10 nm Nanoparticle Ensemble via Vogel – Fulcher Law

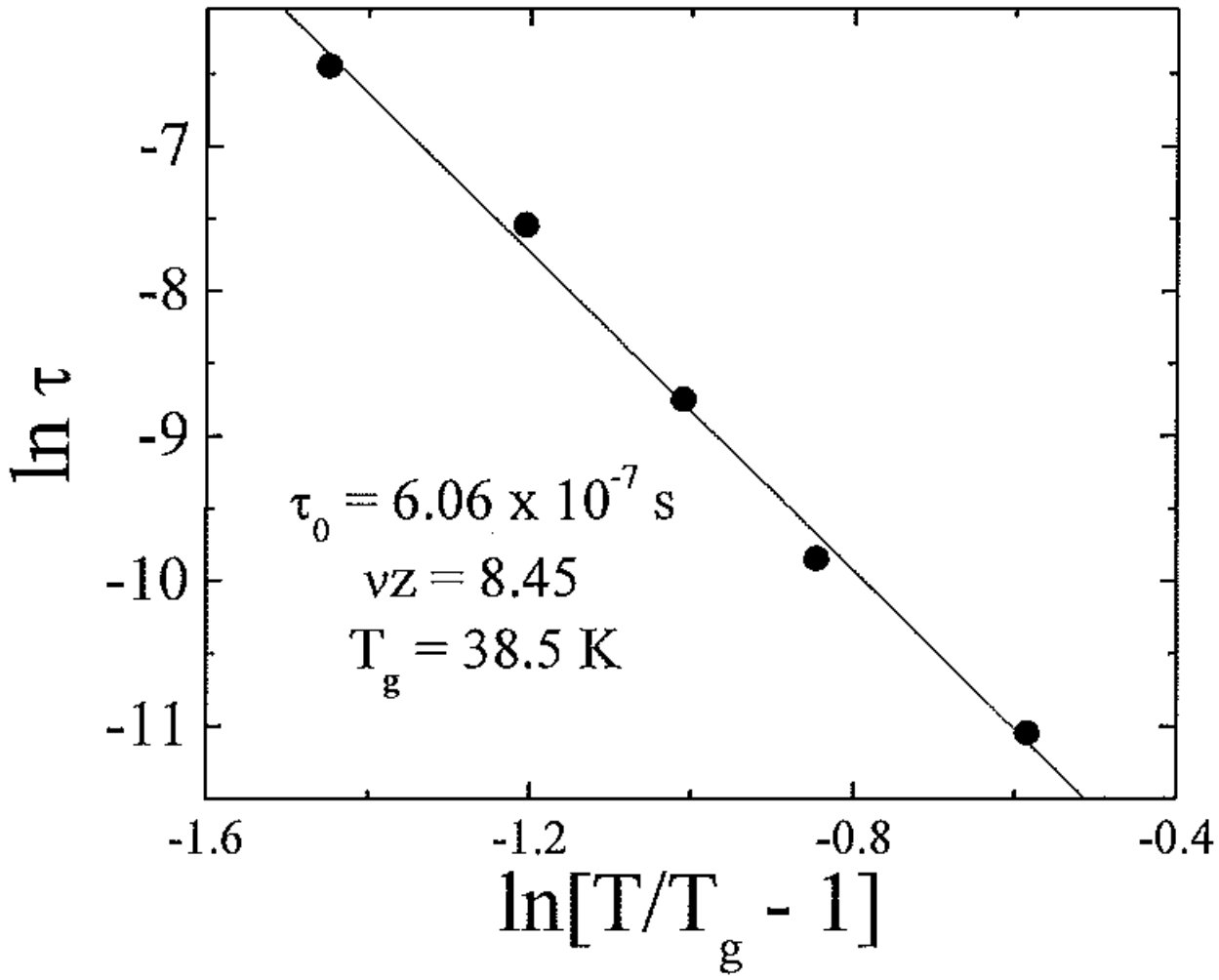

Figure 3.6 – Time Dependence of the Fe_3O_4 Nanoparticle Ensemble via Power Activation Law

Though we can tell the difference between SPB and SSG freezing by fitting data to mathematical models, the data itself is hard to tell apart, as can be seen in figures 3.3 & 3.4. Another issue that arises is the fact that you can also fit either data set to either model, though the values that are used to fit the data may potentially fall outside of allowed physical ranges thus giving validity to whether or not the correct behavior is being detected. This also brings about difficulty in differentiating between the two phenomena. Due to the nature of these phenomena, the energy signature should be quite different between them. This investigation takes the magnetometry measurements performed by Botez et al [21] as a foundation and implements

electron paramagnetic resonance measurements in order to easily differentiate the two phenomena (SPB & SSG).

3.2 SAMPLE PREPARATION

Two commercially produced Fe_3O_4 nanoparticles with an average diameter of 10 nm were procured through NN-Labs, LLC. The magnetite we used was procured in two forms: the first being a powder; the second as a ferrofluid with 10 mg of Fe_3O_4 immersed in 5 mL of toluene as a carrier. Each sample was loaded into its own precision quartz EPR tube.

3.3 ELECTRON PARAMAGNETIC RESONANCE

Electron paramagnetic resonance (EPR) is a technique based on the absorption of electromagnetic radiation, typically in the microwave frequency region, by a paramagnetic sample placed in an external magnetic field [22]. This is done by exciting the electron spins of unpaired electrons. Every electron has a magnetic moment and half integer spin, with the magnetic components $m_s = \pm ½$. When in the presence of an external magnetic field, the electrons align in either a parallel or antiparallel fashion with the field. These alignments have specific energies tied to them due to the Zeeman effect given by:

$$E = m_s g_e \mu_B B_0 \tag{8}$$

where E is the energy, m_s is the spin value, g_e is the g-factor (typically around 2 and equal to 2.0023 for the free electron [23]), μ_B is the Bohr magneton, and B_0 is the strength of the magnetic field. Unpaired free electrons have separation energy of

$$\Delta E = g_e \mu_B B_0 \tag{9}$$

thus implying that splitting of the energy levels is proportional to the magnetic field. Since photons have an energy of $h\nu$, the absorption or emission of a photon at resonance $h\nu = \Delta E$ allow the unpaired electron to move between the two energy levels. The resonance position can then be given by

$$B_0 = \frac{h\nu}{g_e \mu_B} \tag{10}$$

In practice, the frequency of the incident photons is held constant and the magnetic field is varied. Due to the electrons favoring the lower energy state, as can be explained by the Maxwell-Boltzmann distribution, there is a net absorption from the sample which is what becomes converted into the EPR spectrum (Figure 3.7).

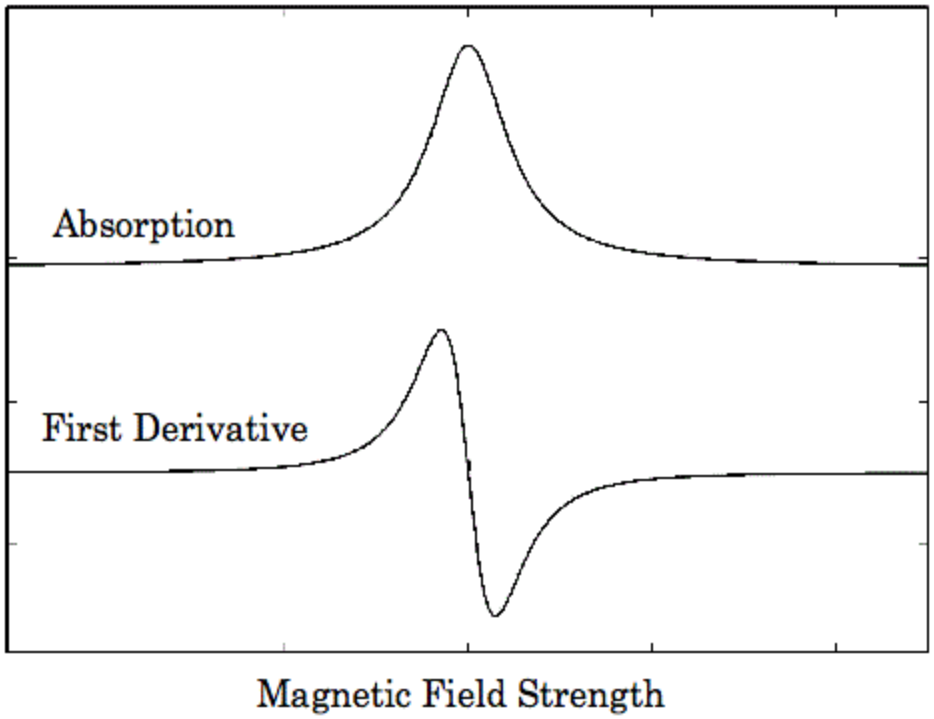

Figure 3.7 – Example of EPR Absorption Spectra and its First Derivative

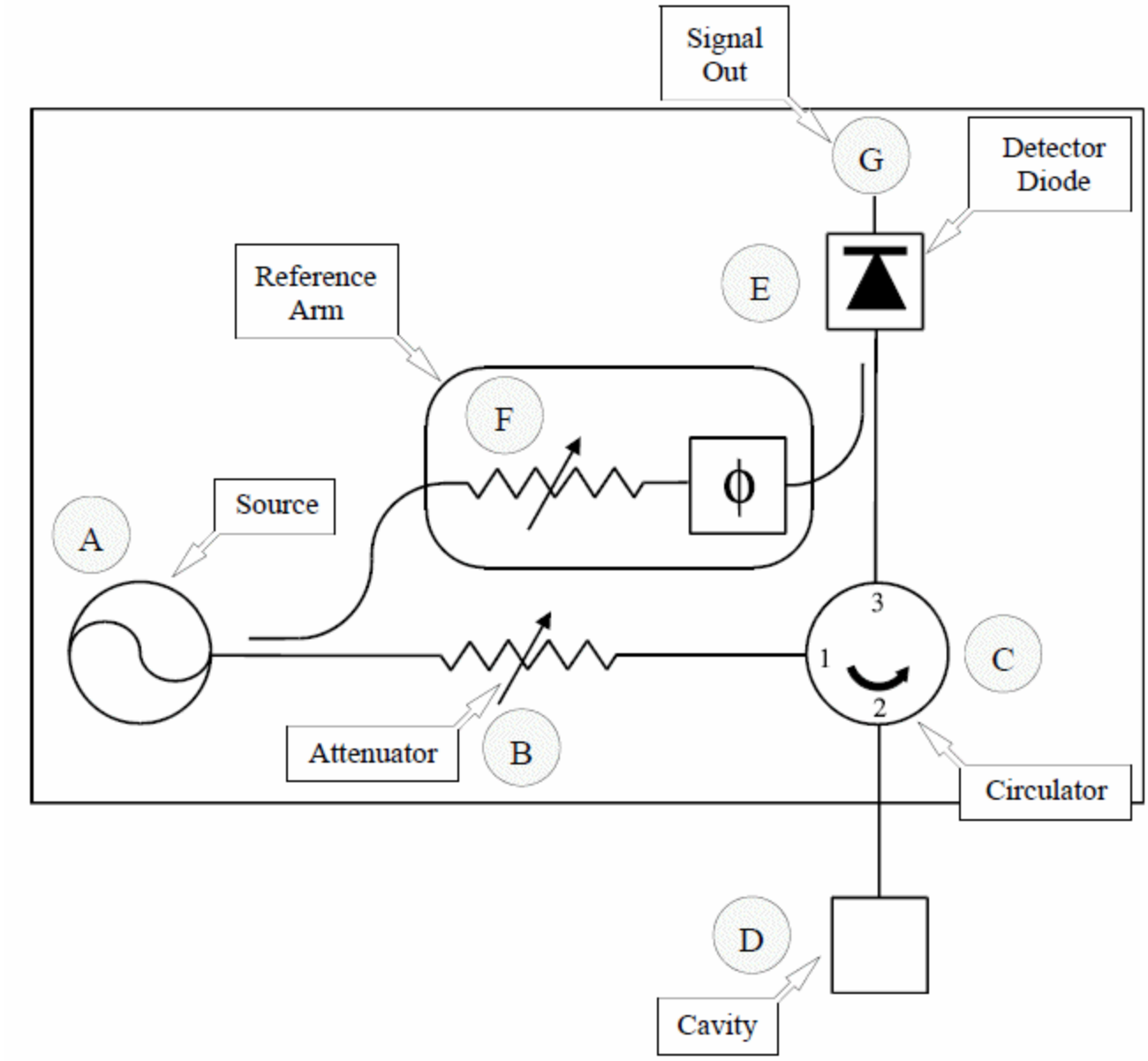

Figure 3.8 – Block Diagram Example of EPR Microwave Bridge

An example of the microwave bridge for an EPR system can be seen in figure 3.8. The microwaves begin at the source marked by point A. The power output from the microwave source cannot be varied easily, so a variable attenuator (point B) is used in order to control the power of the microwave that reaches the sample. A circulator (point C) is in place so the source microwaves only go to the sample (point D), not the detector, and the reflected microwaves go to the detector, not the source. A Schottky barrier diode (point E) is used to convert the reflected

microwave power into an electrical current. The reference arm (point F) taps some of the source microwave power and sends it to the detector diode in order to maintain a proper current for smooth operation. A second attenuator is located there to control the amount of power is sent to the diode detector, as well as a phase shifter to assure the reflected signal combines properly with the supply signal.

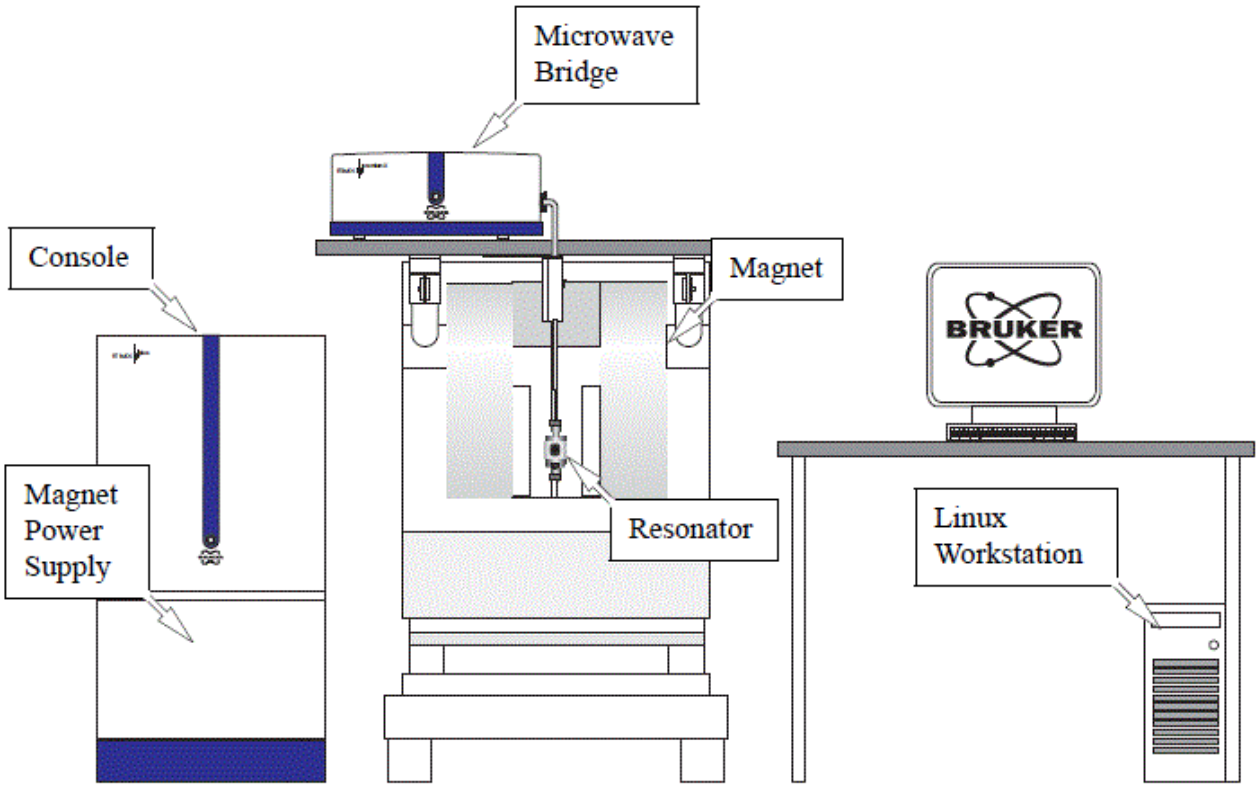

Figure 3.9 – Modules and Components of the Bruker EMXplus Spectrometer

Measurements were carried out on a Bruker EMX-plus X-band spectrometer (Figure 3.9). The microwave source has a constant frequency of 9.398 GHz (X-band). Our Fe_3O_4 powder sample was lowered into the resonator and cooled to 20 K. A scan was then taken with a varying magnetic field from 0 G – 6000 G. We then incremented the temperature by 10 K, allowing ample time (about 10 – 15 minutes) for the sample to come to thermal equilibrium with the resonator chamber, repeating this process until we spanned the 20 K – 120 K temperature range.

Measurements of the ferrofluid sample were then taken in a similar fashion. Before lowering the sample tube into the resonator cavity, it was first bathed in liquid nitrogen to ensure the toluene carrier froze in a glass-like state so as to not to add a bias to our readings. The ferrofluid was then lowered into the resonator cavity and chilled to 20 K where a scan over the 0 G – 6000 G range was then conducted. This was also repeated for every 10 K up to maximum temperature of 120 K.

Chapter 4: Results and Discussion

The first derivative of the EPR absorption spectra for the Fe_3O_4 nanopowder was plotted intensity vs. temperature (Figure 4.1). We then isolated the absorption peak (the line center from the first derivative data) and plotted the absorption peaks vs. temperature (figure 4.2). The slope of the fitted line shows a distinct change in the 40 K – 50 K temperature range. The modulation frequency of the magnetic field for the EPR measurements is 100 kHz. Cross referencing this with the data analyzed from the ac-susceptibility measurements from figure 3.3, we see a correlation with ac-susceptibility peaks, as the peak temperature shifts higher with a higher frequency. Referring back to figure 3.6, the ac-susceptibility data was fitted to the power activation law for strongly interacting systems. The calculated freezing temperature is 38.5 K,

which closely matches the data in figure 4.2.

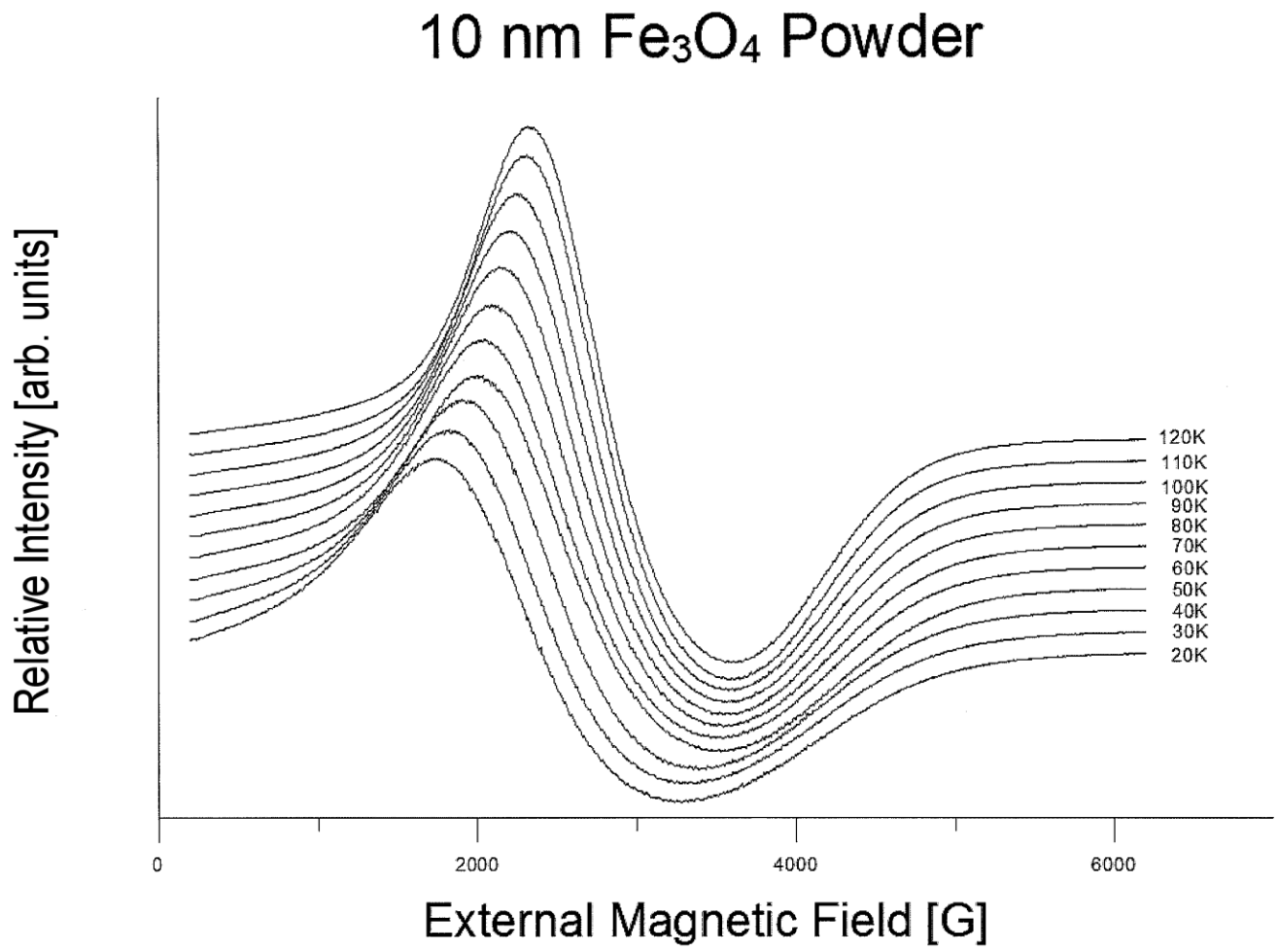

Figure 4.1 – EPR Spectra for Fe_3O_4 10 nm Powder

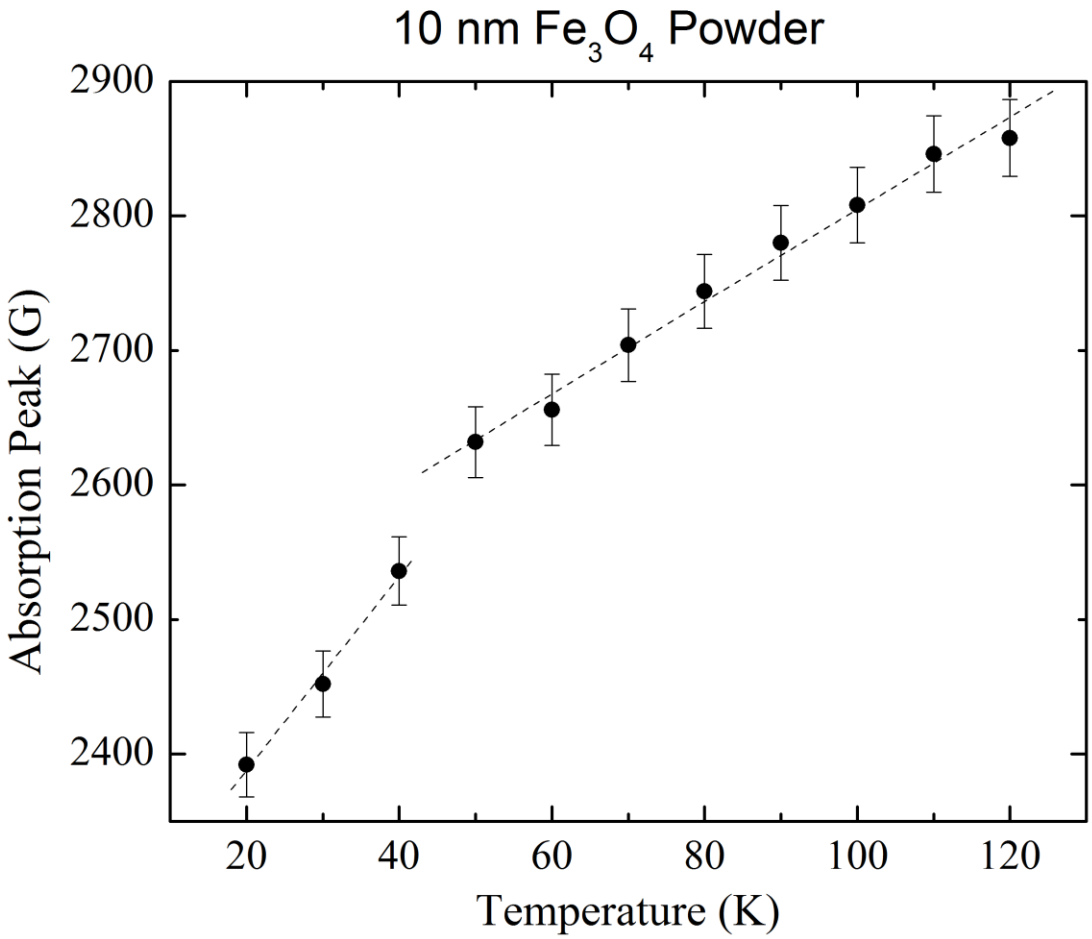

Figure 4.2 – Plot for Absorption Peak vs. Temperature in Powder Sample

Figure 4.3 shows the EPR absorption spectra for the Fe_3O_4 ferrofluid. The line width broadening is clearer to see in the diluted ferrofluid at lower temperatures compared to that of its powder counterpart. The absorption peaks were then plotted against the temperature (figure 4.4). Distinctly different behavior is shown with the ferrofluid compared to the powder. We see a shift in the linewidth at the 80 K mark, and at the 40 K mark where it becomes very broad. The dashed lines merely act as a guide for eye.

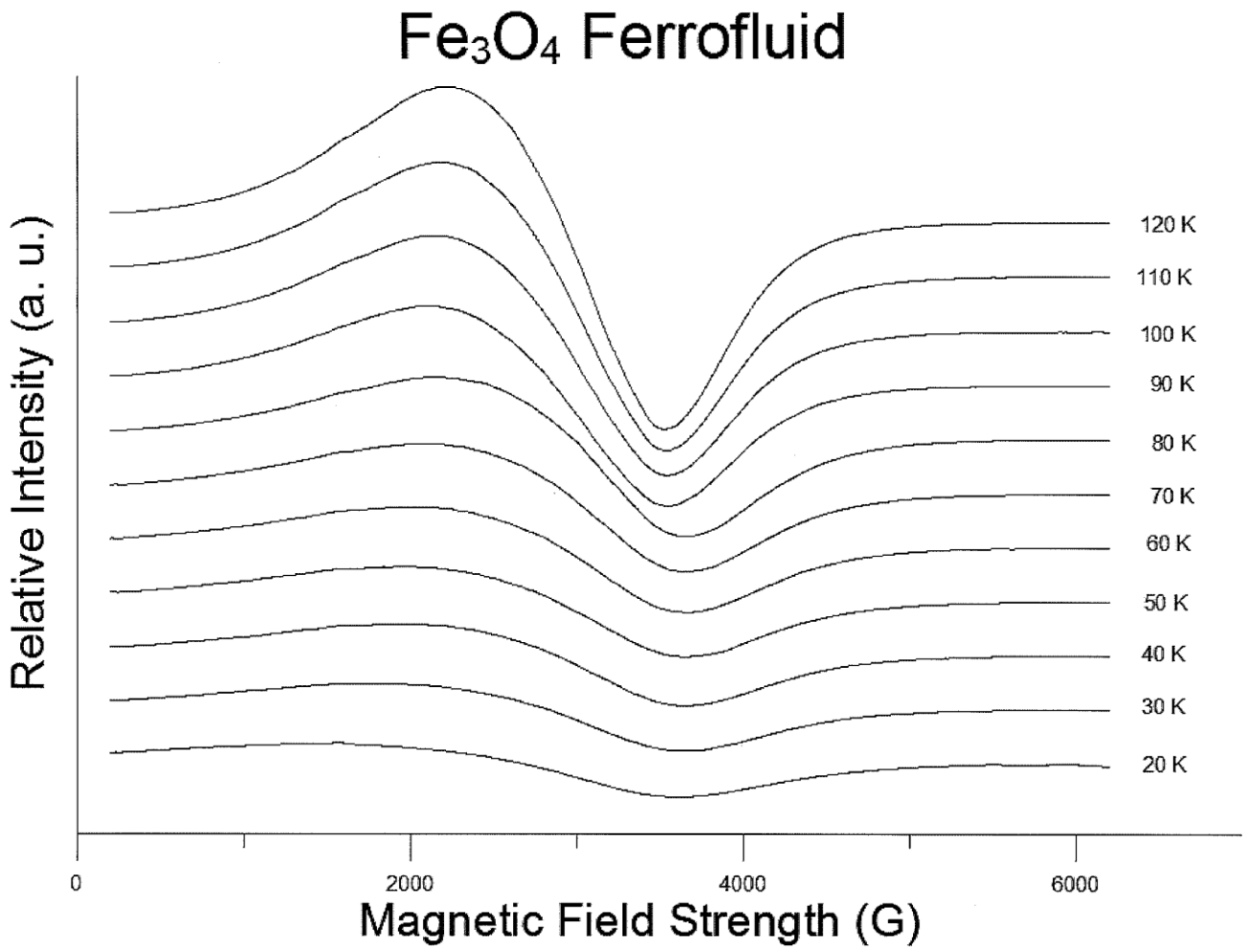

Figure 4.3 – EPR Spectra for Fe_3O_4 10 nm Ferrofluid

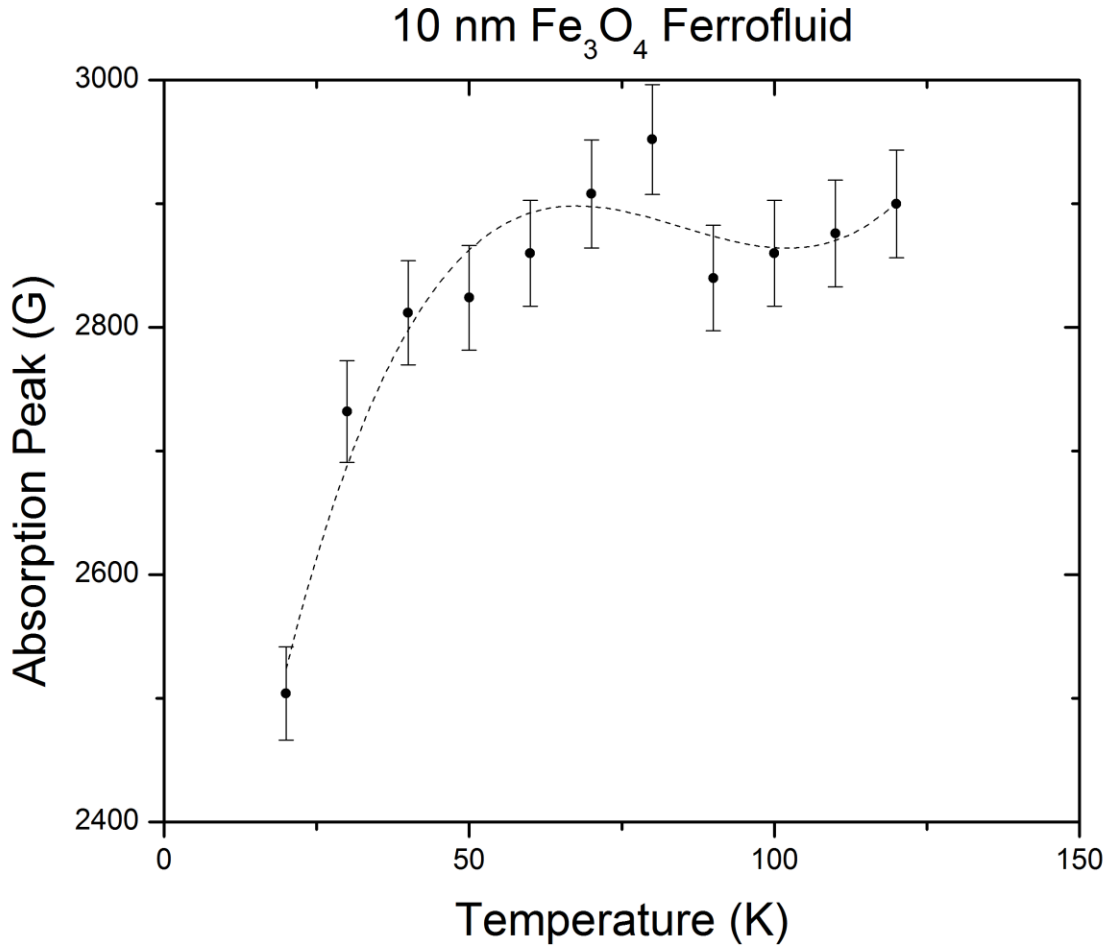

Figure 4.4 – Plot of Absorption Peak vs. Temperature in Ferrofluid Sample

A calculation for ΔH_{PP} (the linewidth from peak to peak measured in Gauss) was then carried out for the powder and ferrofluid samples (figures 4.5 and 4.6). Previous investigations by Koksharov et al describe a linewidth analysis with a noticeable broadening of the linewidth [24]. The narrower linewidth is described as the superparamagnetic resonance signal while the broader linewidth is indicative of ferromagnetic resonance. In figure 4.5, we see what appears to be a phase transition near 40 K with no dramatic change in overall behavior of the linewidth. This may be due to the superspin-glass-like freezing as the frustrated configuration of the spins, caused by dipolar interactions due to the close interparticle distance, may be indicative of a frozen in magnetization. As the powder is cooled while in a zero field environment, we would

expect the SSG configuration to be characteristic of a paramagnetic behavior. In figure 4.6, we see a drastic change in the linewidth behavior below 40 K. This rather broad linewidth is characteristic to ferromagnetic resonance. This would imply the superspins have individually blocked at this lower temperature giving the material a ferromagnetic ordering of the magnetic domains. Therefore, at higher temperatures a narrower linewidth is expected due to the superparamagnetic fluctuations; whereas at lower temperatures the nanoparticles transition to a stable state giving the EPR signals a broader linewidth. This coincides with Koksharov et al [24]. In conclusion, our data provides evidence of EPR measurements to describe superparamagnetic blocking and superspin-glass freezing as an alternative to traditional magnetometry techniques.

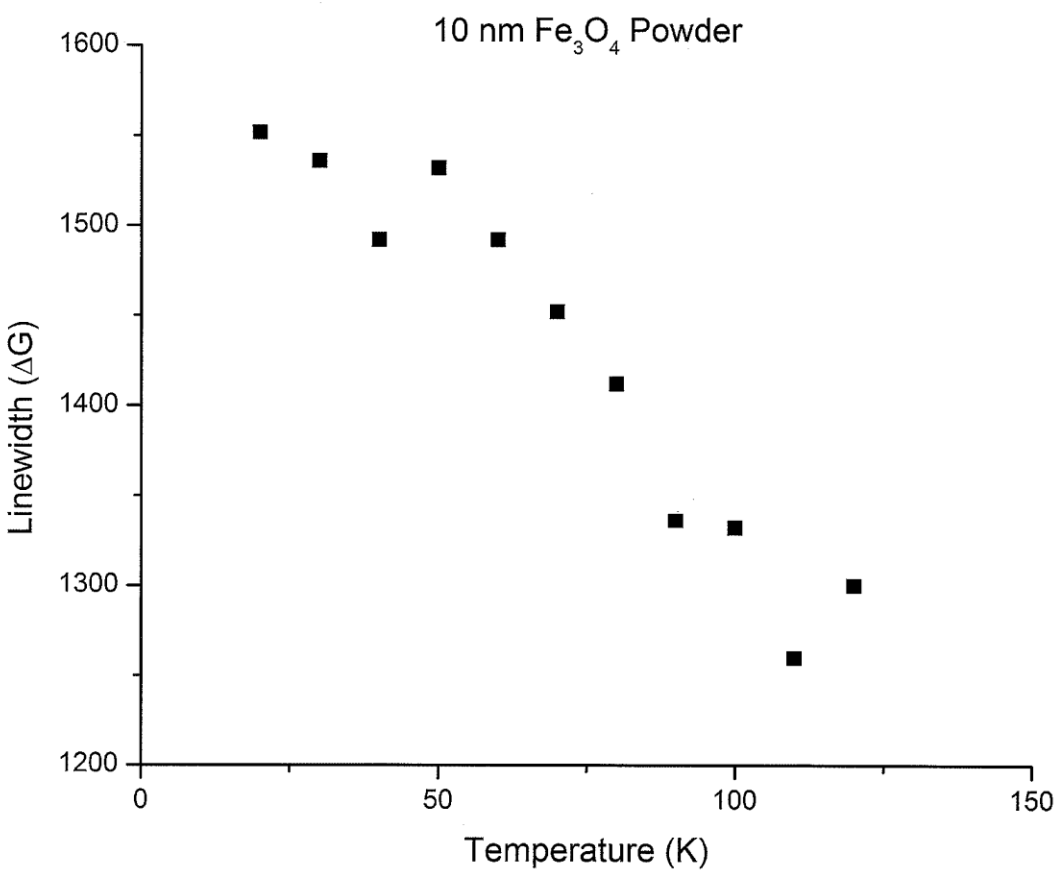

Figure 4.5 – Linewidth vs. Temperature Plot for Fe_3O_4 Nanopowder

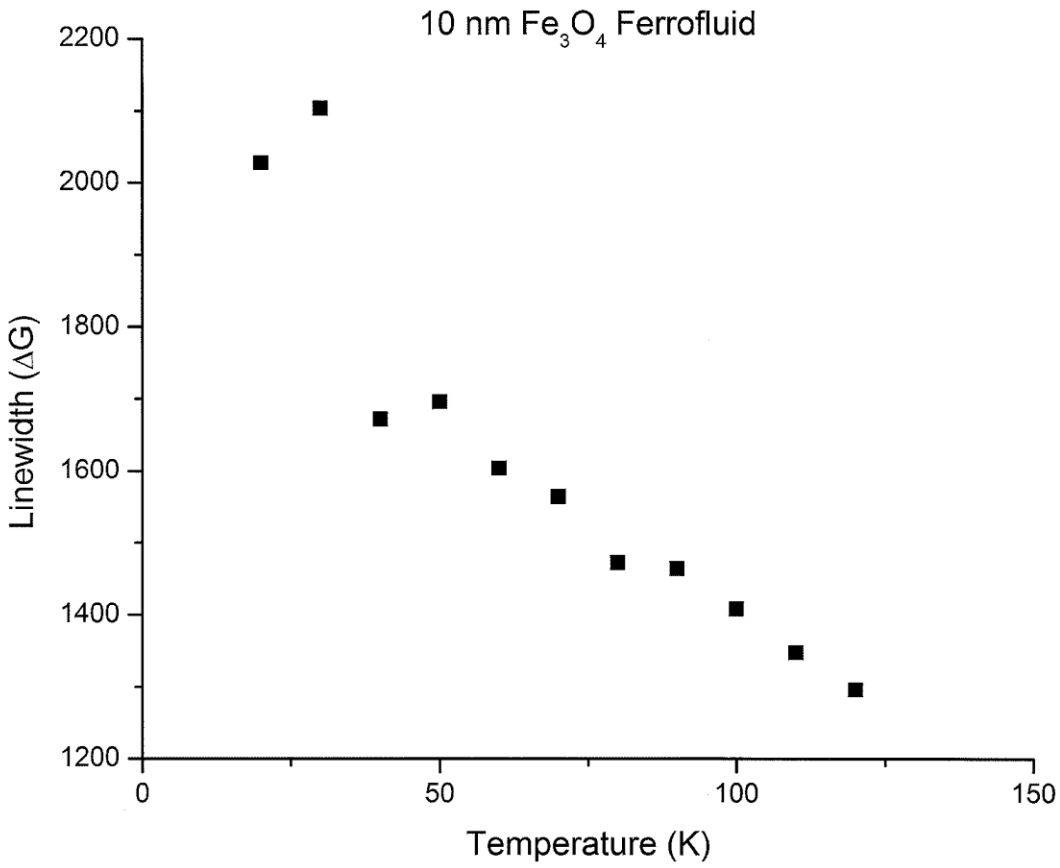

Figure 4.6 – Linewidth vs. Temperature Plot for Fe_3O_4 Ferrofluid

Chapter 5: Conclusions

We studied the superspin dynamics of 10 nm average diameter Fe_3O_4 magnetic nanoparticles using electron paramagnetic resonance in conjunction with DC-magnetization and AC-susceptibility magnetometry. We took our magnetometry data which was modeled using the Vogel – Fulcher activation law and the dynamic scaling power activation law to see the superparamagnetic blocking and superspin glass freezing of magnetite. The AC-susceptibility measurements are difficult to differentiate between the two types of superparamagnetic relaxations without these mathematical modeling techniques.

EPR measurements for a trial set of 10 nm Fe_3O_4 magnetic nanoparticles were then taken in order to show a clear difference between SPB and SSG freezing. This was expected since both phenomena have a distinct difference in their energy scales. The measurements were taken using X-band microwaves over a temperature range of 20 K – 120 K under a varying external magnetic field of 0 G – 6000 G. The first derivative of the absorption spectra for the nano-powder and the ferrofluid did differ from each other. Further analysis was done by plotting the absorption peak vs. temperature as well as the linewidth (peak to peak) vs. temperature. Both presented distinct behavior from each other which coincided with our prior magnetometry measurements as well as the investigations performed by Koksharov et al.

Further work is required to fully classify the EPR approach for classification of superparamagnetic relaxation in these magnetite nanoparticles. An ensemble of various sizes of Fe_3O_4 magnetic nanoparticles ranging from 1 nm – 10 nm at different concentrations of ferrofluid combinations should be measured. This will further explain the size dependence of the superspin relaxation as well as the shift in behavior between SPB and SSG freezing due to the differing interparticle interactions.

References

[1] Natalie A. Frey and Shouheng Sun, *Magnetic Nanoparticle for Information Storage Applications*, CRC Press, (2010)

[2] K. Hayashi et al. *Superparamgnetic Nanoparticle Clusters for Cancer Theranostics Combining Magnetic Resonance Imaging and Hyperthermia Treatment*, Theranostics, Vol. 3, Issue 6, (2013)

[3] W. Lowrie, *Fundamentals of Geophysics*, London: Cambridge University Press, p. 281, (2007)

[4] Sergei P. Gubin, *Magnetic Nanoparticles*, Wiley, (2009)

[5] S. Scheonherr, *The History of Magnetic Recording*, Audio Engineering Society, (2002)

[6] J. T. Mayo et all, *The Effect of Nanocrystalline Magnetite Size on Arsenic Removal*, Science ans Technology of Advanced Materials 8, 71-75 (2007)

[7] Richard J. Harrison et al, *Direct Imaging of Nanoscale Magnetic interactions in Minerals*, Stanford University (2002)

[8] Steve Papell, *US Patent # 3215572,* filed Oct. 9, 1963

[9] W. Voit, D. K. Kim, W. Zapka, M. Muhammed, and K. V. Rao. *Magnetic Behavior of Coated Superparamagnetic Iron Oxide Nanoparticles in ferrofluids*. MRS Proceedings, 676, Y7.8, (2001)

[10] Blaine Brownell, *Matter in the Floating World*, Princeton Architectural Press, pp. 192-199 (2011)

[11] Fowler, Michael, *Historical beginnings of Theories of Electricity and Magnetism*, (1997)

[12] C. P. Bean and J. D. Livingston, J. Appl. Phys. 30 (1959)

[13] K. Binder and A. P. Young, Reviews of Modern Physics 58 (4), 801-976, (1986)

[14] L. Neel, C. R. Hebd, Seances Acad. Sci. 5 (1949)

[15] William Fuller Brown Jr., *Thermal Fluctuations of a Single-Domain Particle*, Physical Review 130 (5): 1677-1686 (1963)

[16] S. Shtrikman and E. Wohlfarth, Phys. Lett. A 85, 467 (1981)

[17] J. L. Tholence, Solid State Comm. 35 (113) (1980)

[18] X. Chen, S. Bendata, O. Petracic, W. Kleemann, S. Sahoo, S. Cardoso, P. P. Freitas, Phys. Rev. B 72, 214439 (2005)

[19] K. Binder, A. P. Young, Phys. Rev. B 29, 2864 (1984)

[20] C. Djurberg, P. Svedlindh, P. Norblad, M. F. Hansen, F. Bodker, S. Mørup, Phys. Rev. let. 79, 5154 (1997)

[21] C. Botez, J. Morris, *AC-Susceptibility Investigations of Superspin Blocking and Freezing in Interacting Magnetic Nanoparticle Ensembles*, Nanotechnology (Under Review)

[22] M. Brustolon and E. Giamello, *Electron Paramagnetic Resonance: A Practitioner's Toolkit*, Wiley (2009)

[23] B. Odom, D. Hanneke, B. D'Urso, G. Gabrielse, *New Measurement of the Electron Magnetic moment Using a One-Electron Quantum Cyclotron*, Physical review Letters 97 (3): 030801 (2006)

[24] Yu. A. Koksharov, S. P. Gubin, I. D. Kosobudsky, M. Beltran, Y. Khodorkovsky, and A. M. Tishin, J. Appl. Phys. 88, 1587 (2000)

Vita

Though born a Californian, Alex D. Price was raised in El Paso from two years of age. He obtained his G.E.D. at the age of 17 and enrolled himself in EPCC. After a few years of bouncing around different majors, he found his calling after taking his first physics course. Shortly after, he transferred to the University of Texas at El Paso where he completed a dual Bachelor's in Physics and Mathematics then proceeded to obtain his Master's in Physics.

During his undergraduate career he worked as a research assistant on Dr. Paul Mason's Astrophysics team, where he enjoyed his time learning about the stars and having fun working at the McDonald Observatory. Upon starting his Master's studies, he switched his research focus to materials where he worked in Dr. Cristian Botez's Crystal Structure and Physical Properties Laboratory. Alex also had the honor of working as a teaching assistant in the Physics department, helping to mold the minds of future scientists and engineers.

Alex hopes to complete his doctorate in Material Science and Engineering where he plans on contributing towards the collective wealth of knowledge in science and engineering.

Permanent address: 910 E. Redd Rd. #244-k
El Paso, TX 79912

This thesis/dissertation was typed by Alex D. Price